AD-A035 609 HUGHES RESEARCH LABS MALIBU CALIF F/G 9/5
CROSSED-FIELD CLOSING SWITCH DEVELOPMENT.(U)
JAN 77 R J HARVEY DAAB07-76-C-1313
UNCLASSIFIED ECOM-76-1313-F NL

1 OF 1
ADA035609

END
DATE
FILMED
3-77

(12)

79

ADA035609

Research and Development Technical Report

ECOM-76-1313-F

CROSSED-FIELD CLOSING SWITCH DEVELOPMENT

Robin J. Harvey

Hughes Research Laboratories
3011 Malibu Canyon Road
Malibu, CA 90265

January 1977

DISTRIBUTION STATEMENT
Approved for public release; distribution unlimited.

Prepared For

ECOM

US ARMY ELECTRONICS COMMAND FORT MONMOUTH, NEW JERSEY 07703

NOTICES

Disclaimers

The findings in this report are not to be construed as an official Department of the Army position, unless so designated by other authorized documents.

The citation of trade names and names of manufacturers in this report is not to be construed as official Government indorsement or approval of commercial products or services referenced herein.

Disposition

Destroy this report when it is no longer needed. Do not return it to the originator.

UNCLASSIFIED

SECURITY CLASSIFICATION OF THIS PAGE (When Data Entered)

19 REPORT DOCUMENTATION PAGE		READ INSTRUCTIONS BEFORE COMPLETING FORM
1. REPORT NUMBER 18 ECOM-76-1313-F	2. GOVT ACCESSION NO.	3. RECIPIENT'S CATALOG NUMBER 9
4. TITLE (and Subtitle) 6 CROSSED-FIELD CLOSING SWITCH DEVELOPMENT.		5. TYPE OF REPORT & PERIOD COVERED Final rept. 8 Janu[redacted] - 31 Dec 76
		6. PERFORMING ORG. REPORT NUMBER
7. AUTHOR(s) 10 Robin J. Harvey		8. CONTRACT OR GRANT NUMBER(s) 15 DAAB07-76-C-1313
9. PERFORMING ORGANIZATION NAME AND ADDRESS Hughes Research Laboratories 3011 Malibu Canyon Road Malibu, CA 90265 172 600		10. PROGRAM ELEMENT, PROJECT, TASK AREA & WORK UNIT NUMBERS 693436.37.161.74.01
11. CONTROLLING OFFICE NAME AND ADDRESS U.S. Army Electronics Command Attn: DRSEL-TL-BG Fort Monmouth, NJ 07703		12. REPORT DATE 11 Janu[redacted]977
		13. NUMBER OF PAGES 30
14. MONITORING AGENCY NAME & ADDRESS (if different from Controlling Office) 12 25p.		15. SECURITY CLASS. (of this report) UNCLASSIFIED
		15a. DECLASSIFICATION DOWNGRADING SCHEDULE

16. DISTRIBUTION STATEMENT (of this Report)

Approved for Public Release: Distribution Unlimited

17. DISTRIBUTION STATEMENT (of the abstract entered in Block 20, if different from Report)

18. SUPPLEMENTARY NOTES

19. KEY WORDS (Continue on reverse side if necessary and identify by block number)

Closing Switch, Arc Discharge, Crossed Field

20. ABSTRACT (Continue on reverse side if necessary and identify by block number)

A triode version of the crossed-field closing switch (CFCS) has been successfully tested at average powers of up to 800 kW (40 kA, 40 kV, 12 μsec Micro Sec pulse width at 80 Hz) for burst durations of 30 sec. Unlike most conventional spark gaps, the arc is initiated from a crossed-field glow discharge and occurs at random locations on a shot-to-shot basis. This uniformly disperses the heat loading and erosion over a relatively large electrode surface area which may then be cooled. END

DD FORM 1 JAN 73 1473 EDITION OF 1 NOV 65 IS OBSOLETE

UNCLASSIFIED

SECURITY CLASSIFICATION OF THIS PAGE (When Data Entered)

172 600

FOREWORD

The full power testing of the crossed-field closing switch was performed at the U.S. Army Electronics Command at Fort Monmouth, New Jersey, in collaboration with Mr. John Creedon and his staff.

TABLE OF CONTENTS

LIST OF ILLUSTRATIONS

I. INTRODUCTION

A. Program Goals and Achieved Levels

The objective of this program was to develop a closing switch for high-energy pulser applications. A triode version of the crossed-field closing switch (CFCS) was chosen for this purpose. Crossed-field devices had previously been shown to have the potential for use as high-average-power closing switches.[1] The key feature which differentiates the CFCS from other spark gaps is that it has no localized trigger electrode to overheat or cause excessive erosion. Instead, the discharge is initiated as a crossed-field discharge which uniformly fills the cylindrical interelectrode space. As the current increases, the current density will eventually exceed a critical level, and a discharge with some of the features of a vacuum arc will form. The location of the "arc," which depends primarily on the surface condition of the electrodes,[2] was found to change randomly from shot to shot. It was one goal of this program to show that the randomization of arc location would enable such a device to be run at an average power of 0.48 MW. In actual tests, the device was shown to operate reliably to at least 0.8 MW and perhaps higher. The other desired electrical characteristics of the switch are compared with the achieved results in Table I. In all cases, the test results either equaled or exceeded the goal levels or were restricted by the capability of the ECOM test facility.

B. Diode versus Triode

According to Reference 1, a magnetic field of about 700 G is required to initiate a discharge at 40 kV. Similar results were found by Boucher and Doehler[3] and by Lutz and Hofmann[4]. More recent results by Harvey and Lutz[5,6] have shown that even more magnetic field may be required to ensure stable operation as the electrodes are conditioned. These devices all had the same "diode" configuration in that the anode and cathode were concentric cylinders.

Table I. Electrical Requirements

Parameter	Goal Levels	Achieved Levels
Peak voltage, kV	40	40*
Peak current, kA	20	40*
Pulse width, μsec	10	12*
Repetition rate, Hz	125	108*
Average current, A	24	40*
Average power, kW	480	800*
Run time	60 sec at 0.5 duty cycle, off for 600 sec. Repeat cycle 6 times	>12 30 sec* runs at or over goal levels. Heat exchange time ~400 sec.
Jitter, μsec	–	<< 1
Lifetime	–	$>6 \times 10^4$ pulses, $>2 \times 10^4$ C
Equivalent resistance	–	0.007 Ω for 800 MW peak power
Trigger pulser power, W	–	< 300

*These maximum levels were determined by external circuit limitations.

T2090

An alternative (triode) approach has been proposed by Lutz[7] which avoids the need for a high magnetic field. A third concentric electrode ("grid") is added which divides the interelectrode space into two parts, as shown in Figure 1. By holding the gride at the cathode potential, with the anode at full voltage, neither gap can be activated by a magnetic field of 100 G. However, raising the grid voltage to about 500 to 1000 V with respect to the cathode initiates a discharge in the grid-cathode gap. By perforating the grid,[8] the plasma from the initial discharge (as small as 3 A) was found to penetrate the grid into the anode space and cause a full-scale discharge to take place. The triode configuration was chosen for the prototype CFCS because it has two advantages over the diode configuration: the power requirements for the magnetic field pulser are reduced by nearly two orders of magnitude, and the start of the discharge is triggered in a more conventional manner with less timing delay and jitter. Prior to this program, the laboratory model triode device shown in Figure 2 was successfully operated as a CFCS in a single-shot mode for over 3600 pulses at 50 kV and 7 kA peak current.

C. Preliminary Experiments

Preliminary high-average-power experiments were performed in collaboration with Mr. John Creedon at the U. S. Army Electronics Command at Ft. Monmouth, New Jersey, using the laboratory model triode device shown above.[9] The results confirmed that the arc tracks are randomly distributed over the active cathode area when the device is operated repetitively in the normal grounded-cathode mode. The thermal run-time limit observed was consistent with theoretical estimates of the time required to overheat the electrodes in either the grounded-cathode or grounded-grid mode. This implies that stabilizing electrode temperature (and gas density) is essential for proper high-average-power CFCS operation. An example of the pulse waveform is shown in Figure 3. The switch was snapped-on for a 50 pulse burst at 60 Hz with a peak current of 5 kA at 24 kV.

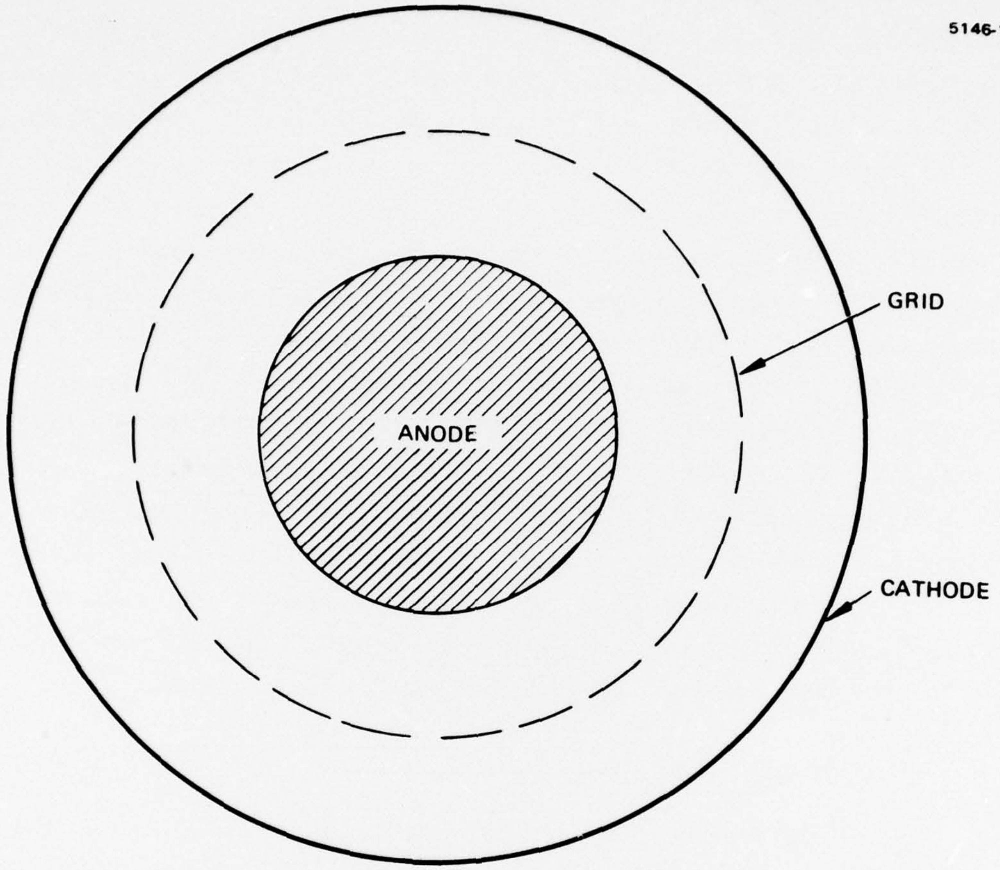

Figure 1. Basic triode configuration of CFCS.

5325-1

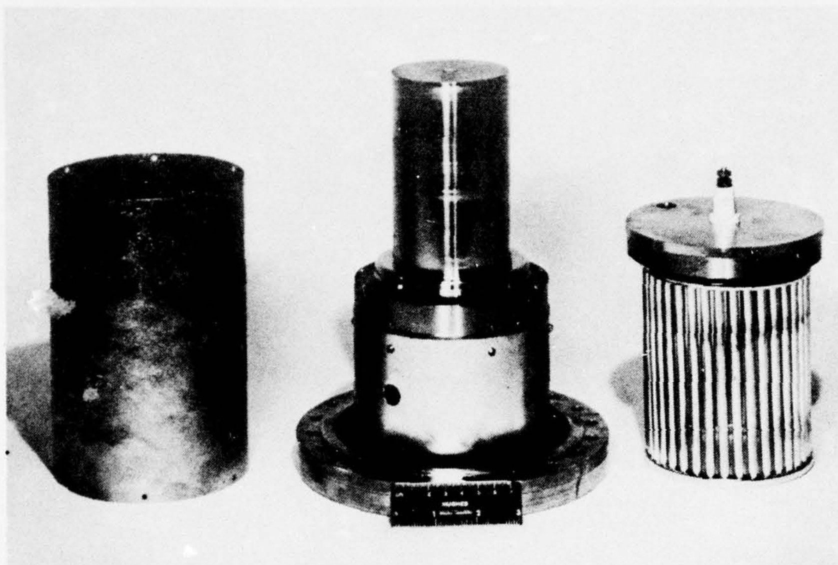

Figure 2. Uncooled triode version of CFCS.

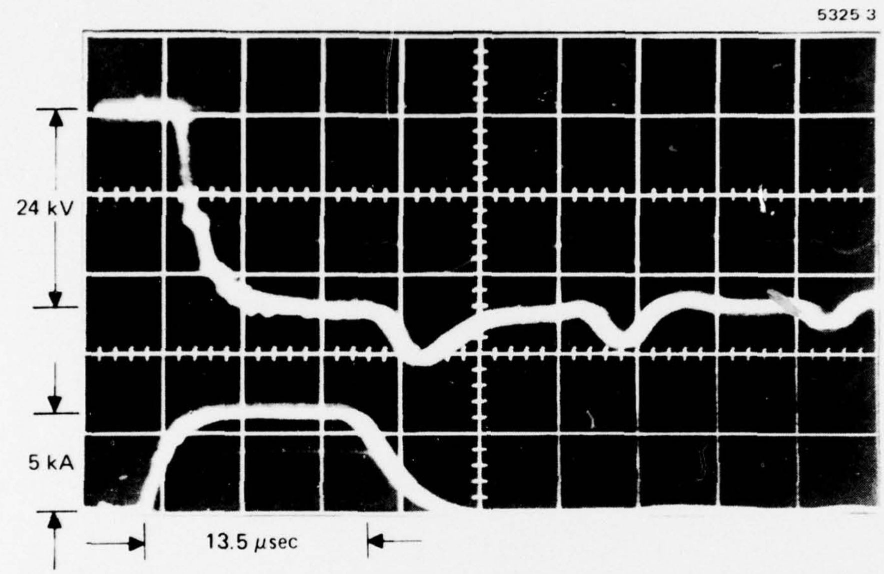

Figure 3. Fifty (50) pulse burst (at 60 Hz), 5 kA, 24 kV.

D. Prototype Design

The design for the full-power prototype CFCS which corrected the above effects is described in Section II. In that design, all three electrodes force cooled; the electrodes are monitored to ascertain the heat loading of the components. The auxiliaries consist of a magnet and grid-trigger pulsing system, a vacuum control system, and a thermal control system. An overview of the switch, the auxiliaries, and the ECOM test facility is shown in Figure 4.

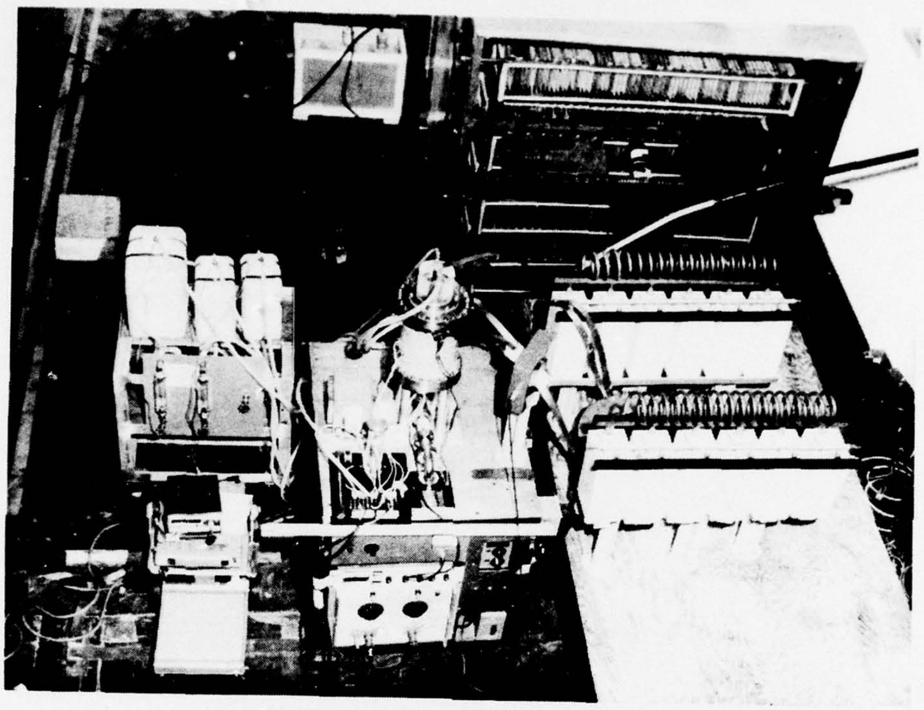

Figure 4. CFCS system and ECOM test facility.

II. THE FULL-POWER PROTOTYPE CFCS

A. Design

The CFCS design is shown in Figure 5. All components exposed to the discharge are OFHC copper, Al_2O_3, or thin-walled metal backed up by water. The cathode is made of thin-walled stainless steel to have a short magnetic field penetration time and also to maintain a low temperature differential between the plasma and the coolant. It forms the vacuum wall and is supported mechanically by vertical ribs which also serve as deflection baffles for the coolant flow. A fiberglass shell is wound over the supporting ribs to enclose the coolant passages. Finally, the magnetic-field coil is wound over the fiberglass shell.

A slotted grid structure is supported at four locations for mechanical stability. Two of the supports also serve as coolant pipes and electrical leads. The hollow Cu anode is cooled by flowing oil through the high-voltage bushing.

The entire anode assembly may be removed for inspection and repair by unbolting the top flange. Likewise, the grid structure is removed by unbolting the lower flange.

The device is designed to withstand a forward voltage in excess of 70 kV under vacuum; it has a natural Paschen breakdown pressure limit of 85 mTorr of He at 40 kV. The normal operating pressure is about 60 mTorr of He.

B. Auxiliaries

The trigger pulsing system is diagrammed in Figure 6. It consists of three components. At the top is the magnetic field pulser, which is resonantly pulse charged and has a resonant flyback inductor to reduce the net charging current. The grid trigger time-delay circuitry (in the center of the diagram) senses a time point equivalent to the peak magnetic field in the coil (about 150 G) and fires the SCR of the grid pulser at the bottom. The grid pulser, in turn, supplies a 600 V, 80 A pulse to drive the grid circuit transformer of the CFCS.

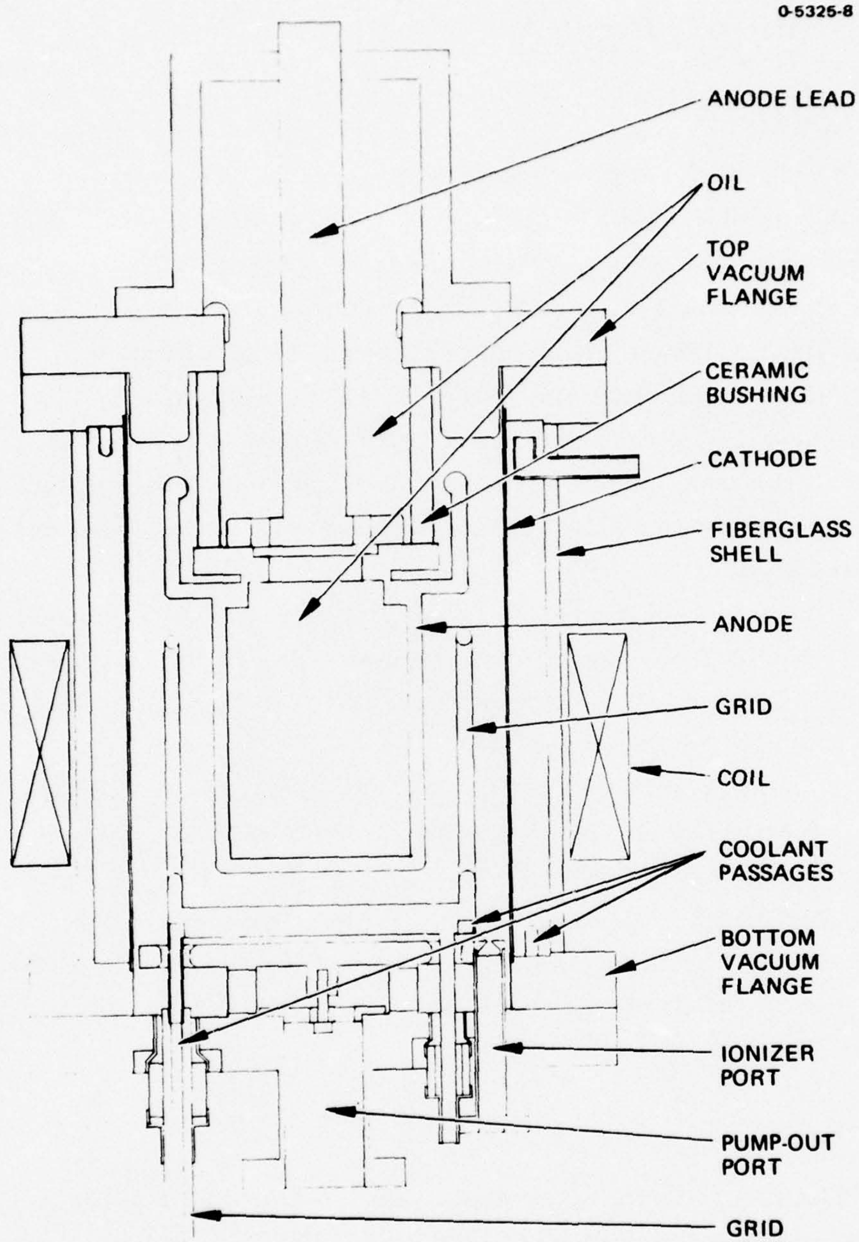

a Side view

Figure 5. High average power prototype CFCS design.

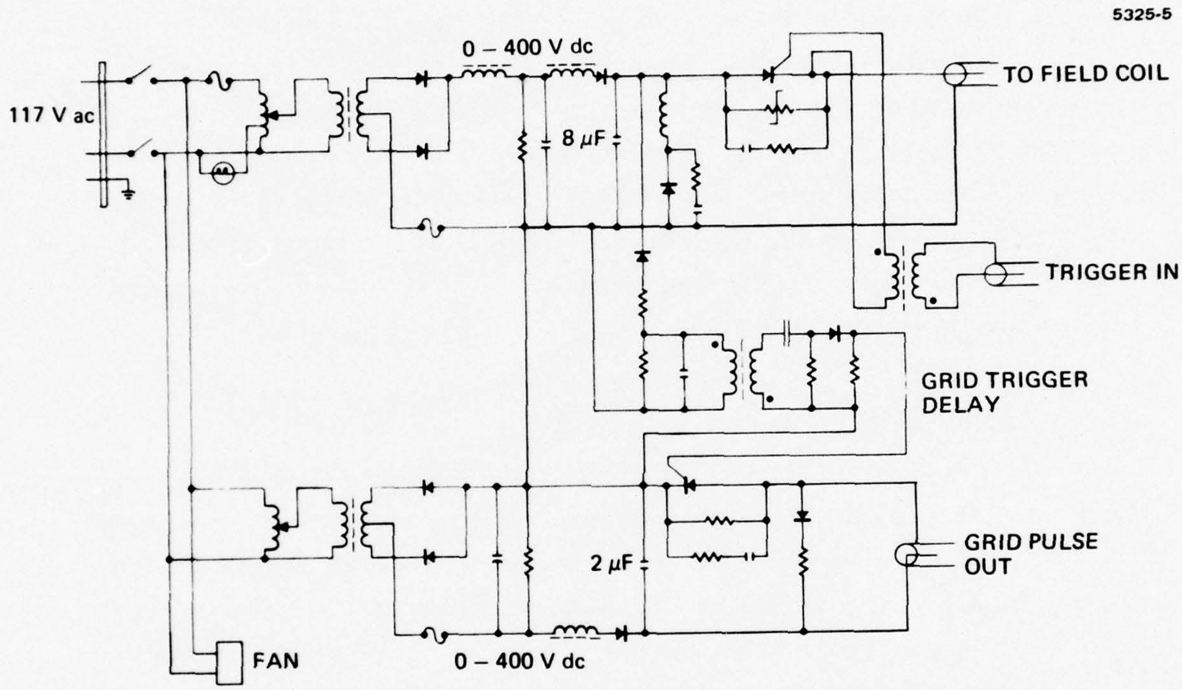

Figure 6. Trigger pulsing system.

The system may be operated from 0 to 125 Hz. The total trigger energy required was found to be <2 J/pulse.

A feedback-controlled vacuum leak valve was initially supplied with the CFCS to maintain a constant He pressure during the testing. The leak valve failed to close properly early in the testing phase. Subsequently, a manually operated leak valve was used to refill the switch in between test runs.

The temperature control system was assembled on a cart. It is composed of three electrically isolated sets, each containing storage containers, pumps, throttle valves, flow meters, and hoses. A digital thermometer monitors the temperature change of the coolant (H_2O or transformer oil) as it enters and leaves the electrodes. The system enables an accurate measurement of both the heat loading and instantaneous temperature of the electrode.

C. Test Circuit

Although the CFCS is capable of operating in either a grounded-grid or a grounded-cathode mode, only the grounded-cathode mode has been tested at full power. The test circuit is shown in Figure 7. The pulse-forming network (PFN) is resonantly charged through the 1.5 H choke. The grid pulser charges the 0.01 μF capacitor to about 2 kV in 1.7 μsec. This is sufficient to discharge the capacitor into the grid-cathode gap, which then transfers plasma to the anode-cathode gap. This results in an anode voltage fall time $\lesssim 0.1$ μsec. The PFN then drives the main discharge current pulse through the switch into a matched resistive load. Two 1 Ω PFNs were used either separately or in parallel as 0.5 Ω.

The pulse rise time was limited to about 1.4 μsec by the lead inductance between the switch and the rest of the circuit. The pulse width (FWHH) was about 12 μsec. The resonant recharge time of the PFN was 8 msec and was independent of the pulse repetition rate.

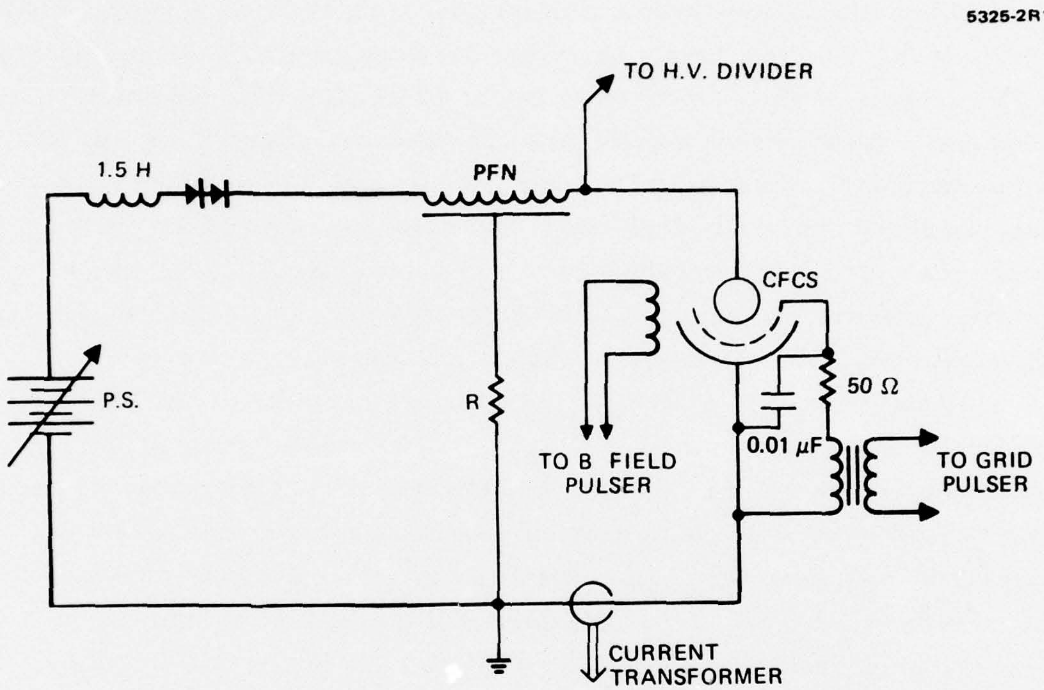

Figure 7. Test circuit.

III. EXPERIMENTAL RESULTS

A. Electrical

The performance of the device has been characterized by a marked and steady improvement in its operating stability with increasing peak power. The test levels have thus far been limited to 30 sec bursts at peak currents of 40 kA, peak voltages of 40 kV, and 12 μsec pulse widths at a repetition rate of 80 Hz. The characteristic 40 kA current pulse waveform is shown in Figure 8. Approximately 16 pulses are superimposed on the oscillogram. These were taken midway during a run. The upper trace was obtained from a resistive divider, which served to determine only the initial PFN voltage. The actual voltage waveform was equivalent to that shown in Figure 3.

Operation at this level yields an average power of 800 kW to the 0.5 Ω load at 40 A average current (1200 A rms). Although a fundamental upper limit in the switched power must exist, no indication of it has yet been observed. During the entire test period, only one "kick-out" was detected. This was at an intermediate power level and may have been related to a failure in the auxiliary equipment.

The present average power limit was set by the power supply, which was run well over its normal rating of 30 A average current. The resonant charging network voltage-recovery rate, however, was equivalent to 125 Hz operation. Repetition rates of up to 108 Hz were demonstrated using a 1 Ω load at 24 A average current (20 kA, 40 kV, 11.4 μsec pulse width) at an average power of 490 kW. The run time and the repetition rate were limited by overheating of the load, and the voltage was limited by the PFN rating.

B. Thermal

The thermal loadings of the three electrodes were monitored calorimetrically using the pumped coolant temperature rise. The net effective cathode voltage drop was found, by this means, to vary with the peak switch power, falling smoothly from 400 ± 25 V at 29 MW to 115 ± 5 V at 800 MW. No repetition rate dependence was observed.

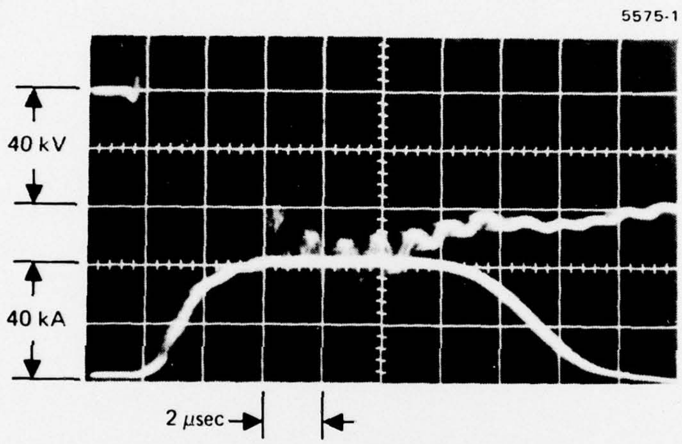

Figure 8.
CFCS operation at: 800 kV average power to load, 800 MW peak power, 80 Hz, and 40 A average current (1240 A rms). Upper trace: resistive divider (dc only), lower trace: switched current pulse wave form; 0.2 sec exposure during 30 sec run.

Similarly, it was found that the grid and anode voltages were 78 ± 6 V and 53 ± 10 V, respectively, and were independent of the peak power or the repetition rate. This information is consistent with earlier, but less accurate, voltage drop measurements made on a diode version of the CFCS operated in a single-shot mode.[2] The estimated temperature rise of either the anode or the grid following a 30 sec run at 0.8 MW is about 90°C. The temperature rise of the cathode is lower (~25°C) due to the high heat capacity of the cooling rater in contact with the rear surface of the cathode. The e-folding time required to transfer the electrode heat to the thermal baths was approximately 6 to 8 min.

C. Pressure

Gas cleanup was observed to depend strongly on peak power, falling as the voltage drop falls. Operation at lower peak power and high repetition rate tends to be unstable without any active pressure control. At 500 MW and above, the pressure was found to stabilize within the normal operating range after the first few seconds of operation.

D. Inverse Clipping

Inverse clipping was observed on a few percent of the pulses. No obvious causal relationships with current, pulse repetition frequency, conditioning time, or pressure were seen; no forward voltage recovery problem was observed (either with or without inverse clipping).

E. Life

Following the conduction of more than 2×10^4 C of charge in about 6×10^4 pulses, the anode of the tube was disassembled from the remainder of the tube and the interior of the device was inspected. No evidence of accelerated wear (or other possible life-limiting effects) was seen. The site of the inverse clipping conduction was found to be localized at the anode's upper shoulder. This created no obvious problems to the tube. Otherwise, the arc-track activity was spread out uniformly over the areas which were originally designed to handle the current. The tube was then reassembled and has since been operated for more than three 30 sec runs.

IV. SUMMARY

The CFCS has been shown to operate reliably at average powers up to 0.8 MW, peak currents up to 40 kA, voltage up to 40 kV, and pulse repetition frequencies up to at least 108 Hz. The upper limits of the peak current, peak voltage, and repetition rate have not yet been established. Since the maximum switchable power varies as the product of these three parameters, it is reasonable to assume that this power limit is in excess of the 0.8 MW reported herein. Likewise, the life limit of the device has not been determined but it is likely to be considerably longer than the present test limit of 20,000 C.

There are two practical limitations to optimum performance in an arbitrary system. The first is the thermal heat loading of the electrodes already described. This is tractable by conventional techniques and will impact the size, weight and duty cycle of the device. The second is the control of the He gas pressure. The stability of the gas pressure was found to be a function of peak current. At currents below about 10 kA, the gas cleanup rate is rapid, presumably due to conduction taking place in a glow-discharge mode. At high currents, the cleanup rate is lower. Relatively little cleanup was observed at the highest current, where the effective conduction voltage drop was low.

Although the conduction mechanism has many features of a vacuum arc, it does not exhibit a sharp glow-to-arc transition at a fixed current density. Also, the voltage drop (between 246 and 530 V) is considerably higher than that of a classical vacuum arc[10] and only 10 to 20% of the excess may be accounted for by resistive losses. Since a similar result has also been observed with diode CFCS,[1] some care must be taken in interpreting the discharge to be an arc.

REFERENCES

1. M.A. Lutz, R. J. Harvey, H. Alting-Mees, "Feasibility of a High Average Power Crossed-Field Closing Switch," IEEE Trans. Plasma Sci. PS-4 118 (June 1976).

2. M.A. Lutz, "The Glow-to-Arc Transition – Critical Review" IEEE Trans. Plasma Sci. PS-2 1, 11 (March 1974).

3. G. Boucher and O. Doehler, "The Artatron – High-Power Switching Device" 3rd Symposium on Engineering Problems in Thermo-Nuclear Research, Munich, June 22-24, 1964.

4. M.A. Lutz and G.A. Hofmann, "The Gamitron – A High Power Crossed-Field Switch Tube for HVDC Interruption," IEEE Trans. Plasma Sci. PS-2 1, 11 (March 1974).

5. R.J. Harvey and M.A. Lutz, "High Voltage Ignition of a Crossed-Field Discharge," Proc. 12th Int. Conf. Phenomenon on Ionized Gases, Part 1, p. 88, Eindhoven, The Netherlands, Aug. 18-22, 1975.

6. R.J. Harvey and M.A. Lutz, "High Power On-Off Switching with Crossed-Field Tubes," IEEE Trans. Plasma Sci. PS-4 4, 210 (December 1976).

7. M.A. Lutz, Pat. Pending.

8. M.A. Lutz and R.J. Harvey, Pat. Pending.

9. R.J. Harvey, "Crossed-Field Closing Switch Development," semi-annual report 1/8/76 – 7/7/76, prepared for U.S. Army Electronics Command, HISA-FM-923-76, Sept. 1976.

10. M.P. Reece, Nature 181 475 (Feb. 1958).

DISTRIBUTION LIST

Copies	
12	Defense Documentation Center ATTN: DDC-TCA Cameron Station (Bldg. 5) Alexandria, VA 22314
1	Code R123, Tech Library DCA Defense Comm. Engrg. Ctr. 18t0 Wiehle Ave. Reston, VA 22090
1	Defense Communications Agency Technical Library Center Code 205 (P.A. TOLOVI) Washington, DC 20305
1	Office of Naval Research Code 427 Arlington, VA 22217
1	Director Naval Research Laboratory ATTN: Code 2627 Washington, DC 20375
1	Commander Naval Electronics Laboratory Center ATTN: Library San Diego, CA 92152
1	CDR, Naval Surface Weapons Center White Oak Laboratory ATTN: Library, Code WX-21 Silver Spring, MD 20910
1	Rome Air Development Center ATTN: Documents Library (TILD) Griffiss AFB, NY 13441
1	Los Alamos Scientific Laboratory Group AP-1 (Mr. W. Willis) Mail Station 566 Los Alamos, NM 87545
1	Los Alamos Scientific Laboratory ATTN: Mr. Roger Warren (Group CTR-9 MS-464) P. O. Box 1663 Los Alamos, NM 87544

Copies	
1	Cdr., US Army Missile Command Redstone Scientific Info Center ATTN: Chief, Document Section Redstone Arsenal, AL 35809
1	Commander US Army Missile Command ATTN: DRSMI-RE (Mr. Pittman) Redstone Arsenal, AL 35809
3	Commandant US Army Aviation Center ATTN: ATZQ-D-MA Fort Rucker, AL 36362
1	Director, Ballistic Missile Defence Advanced Technology Center ATTN: ATC-R, PO Box 1500 Huntsville, AL 35807
1	Commander US Army Intelligence Center & School ATTN: ATSI-CD-MD Fort Huachuca, AZ 85613
1	Commander HQ Fort Huachuca ATTN: Technical Reference Div. Fort Huachuca, AZ 85613
2	Commander US Army Electronic Proving Ground ATTN: STEEP-MT Fort Huachuca, AZ 85613
1	Commander USASA Test & Evaluation Center ATTN: IAO-CDR-T Fort Huachuca, AZ 85613
1	Deputy for Science & Technology Ofc. Assist. Sec. Army (R&D) Washington, DC 20310
1	HQDA (DAMA-ARP/DR. F. D. Verderame) Washington, DC 20310

Copies	
1	Commandant US Army Signal School ATTN: ATSN-CTD-MS Fort Gordon, GA 30905
1	Commandant US Army Ordnance School ATTN: ATSL-CD-OR Aberdeen Proving Ground, MD 21005
1	CDR, Harry Diamond Laboratories ATTN: Library 2800 Powder Mill Road Adelphi, MD 20783
1	Director US Army Ballistic Research Labs ATTN: DRXBR-LB Aberdeen Proving Ground, MD 21005
1	Harry Diamond Laboratories, Dept. of Army ATTN: DRXDO-RCB (Dr. J. Nemarich) 2800 Powder Mill Road Adelphi, MD 20783
1	Director US Army Materiel Systems Analysis Acty. ATTN: DRXSY-T Aberdeen Proving Ground, MD 21005
1	CDR, US Army Aviation Systems Command ATTN: DRSAV-G PO Box 209 St. Louis, MO 63166
1	CDR, US Army Research Office ATTN: DRXRO-IP PO Box 12211 Research Triangle Park, HC 07709
1	Commandant US Army Inst. for Military Assistance ATTN: ATSU-CTD-MO Fort Bragg, NC 28307
1	Commandant US Army Air Defense School ATTN: ATSA-CD-MC Fort Bliss, TX 79916

Copies	
1	Commander US Army Nuclear Agency Fort Bliss, TX 79916
1	Commander, HQ MASSTER Technical Information Center ATTN: Mrs. Ruth Reynolds Fort Hood, TX 76544
1	Commander, DARCOM ATTN: DRCDE 5001 Eisenhower Ave. Alexandria, VA 22333
1	CDR, US Army Security Agency ATTN: IARDA-IT Arlington Hall Station Arlington, VA 22212
2	Commander US Army Logistics Center ATTN: ATCL-MC Fort Lee, VA 22801
1	Chief OFC of Missile Electronic Warfare Electronic Warfare Lab, ECOM White Sands Missile Range, NM 88002
1	Chief Intel Materiel Dev. & Support Ofc. Electronic Warfare Lab, ECOM Fort Meade, MD 20755
	Commander US Army Electronics Command Fort Monmouth, NJ 07703
	1 DRSEL-PL-ST 1 DRSEL-NL-D 1 DRSEL-WL-D 1 DRSEL-VL-D 3 DRSEL-CT-D 1 DRSEL-BL-D 1 DRSEL-TL-DT 3 DRSEL-TL-BG 1 DRSEL-TL-BG (Ofc. of Record) 1 DRSEL-TE 1 DRSEL-MA-MP

Copies

Commander
US Army Electronics Command
Fort Monmouth, NJ 07703 (Cont.)

1 DRSEL-MA-MP
2 DRSEL-MS-TI
1 DRSEL-GG-TD
1 DRSEL-PP-I-PI
1 DRSEL-GS-H
1 DRSEL-CG(Mr. Doxey)
2 DRSEL-PA
1 DRSEL-RD
1 DRSEL-TL-D
1 USMC-LNO
1 TRADOC-LNO

1 CINDAS
Purdue Industrial Reserach Park
2595 Yeager Road
W. Lafayetter, IN 47096

2 MIT - Lincoln Laboratory
ATTN: Library (RM A-082)
PO Box 73
Lexington, MA 02173

1 NASA Scientific & Tech Info Facility
Baltimore/Washington INTL Airport
PO Box 8757, MD 21240

1 National Bureau of Standards
Bldg. 225, Rm. A-331
ATTN: Mr. Leedy
Washington, DC 20231

2 Advisory Group on Electron Devices
201 Varick Street, 9th Floor
New York, NY 10014

2 Advisory Group on Electron Devices
ATTN: Secy, Working Group D (Lasers)
201 Varick Street
New York, NY 10014

1 TACTEC
Battelle Memorial Institute
505 King Avenue
Columbus, OH 43201

Copies	
1	Metals and Ceramics Inf. Center Battelle 505 King Avenue Columbus, OH 43201
1	Fusion Industries, Inc. ATTN: Mr. Vernon Smith PO Box 3183 Dallas, Texas 75231
1	General Electric Co., HMED ATTN: Mr. C. J. Eichenauer, Jr. Court Street Syracuse, NY 13201
1	RCA - MSR Division ATTN: Mr. Duard Pruitt Boston Landing Road Moorestown, NJ 08057
1	Mr. Richard Verga AFAPL/POD-1 Wright Patterson AFB, OH 45433
1	Mr. Charles Cason USA Missile Command AMSMI-RHS Redstone Arsenal, AL 35809
1	Dr. George Dezenberg USA Missile Command AMSMI-RHS Redstone Arsenal, AL 35809
1	Mr. J. O'Loughlin Weapon Lab Kirtland AFB, NM 87117
1	Dr. M. F. Rose Naval Surface Weapon Center White Oak Lab Silver Spring, MD 20910
1	Dr. G. Langerbeam LLL Box 808 Livermore, CA 94550

Copies

1		Mr. Bobby Gray Rome Air Development Center OCTP Griffis AFB, NY 13440
1		Mr. A. E. Gordon ITT Electron Tube Division Box 100 Easton, PA 18042
1		Mr. Richard Fitch Maxwell Laboratories, Inc. 9244 Balboa Avenue San Diego, CA 92123
1		Mr. Harlan Aslin Physics International 2700 Merced Street San Leandro, CA 94577
1		Mr. John Moriarty Raytheon Missile Division Hartwell Road Bedford, MA 01730
1		Mr. R. A. Gardenghi Westinghouse Defense & Electronic System Center Friendship International Airport Box 1897 Baltimre, MD 21203
1		Mr. Robert Feinberg Avco Everett Research Lab 2385 Revere Beach Parkway Everett, MA 02149
1		Mr. David U. Turnquist EG&G Inc. 35 Congress Street Salem, MA 01970
1		Mr. A. Wickson Airesearch Manufacturing Co. 2525 W. 190th Street Torrance, CA 90509
2		Dr. L. Amstutz USA Mobility Equipment R&D Command DRXFB-EA Fort Belvoir, VA 22060

Copies

2	Dr. J. Hammond USA Missile Command High Energy Laser System Project Office AMCPM-HEL Redstone Arsenal, AL 35809
2	Mr. J. Heckl Naval Surface Weapon Center White Oak Lab Code WA -13 Silver Spring, MD 20910